Geomechanics and Engineering, Vol. 5, No. 1 (2013) 57-70
DOI: http://dx.doi.org/10.12989/gae.2013.5.1.057

Interpretation of coefficient of consolidation from CRS test results

Rui Jia*[1], Jinchun Chai[2] and Takenori Hino[1]

[1] *Institute of Lowland and Marine Research, Saga University, Saga, Japan*
[2] *Department of Civil Engineering and Architecture, Saga University, Saga, Japan*

(Received April 24, 2012, Revised October 11, 2012, Accepted October 27, 2012)

Abstract. Constant rate of strain (CRS) consolidation tests were conducted for undisturbed Ariake clay samples from three boreholes in Saga Plain of Kyushu Island, Japan. The coefficients of consolidation (c_v) were interpreted from the CRS test results by small- and large-strain theory. Large-strain theory was found to interpret smaller c_v values and less strain rate effect on c_v than that by small-strain theory. Comparing the theoretical strain distributions within a soil specimen to those obtained by numerical simulation shows that the small-strain theory can be used only for the dimensionless parameter $c_v / \dot{\varepsilon} H_0^2 \geq 50$ (where $\dot{\varepsilon}$ is strain rate and H_0 is the specimen height), and the large-strain theory can be used for a larger range of strain rates. Applying the criterion to undisturbed Ariake clay with a c_v value of about 1×10^{-7} m^2/s, it is suggested that the large-strain theory should be adopted for calculating the c_v value when $\dot{\varepsilon} > 0.03$%/min.

Keywords: constant rate of strain (CRS); coefficient of consolidation; strain rate effect; large-strain theory

1. Introduction

The constant rate of strain (CRS) consolidation test is a standard way of determining the consolidation characteristics of clayey soils. CRS tests have been performed on different natural clays (e.g., Vaid *et al.* 1979, Graham *et al.* 1983, Leroueil *et al.* 1985, Leroueil 1988, Yune and Chung 2005, Tanaka *et al.* 2006, Bo *et al.* 2008, Moriwaki and Satoh 2009, Bo *et al.* 2010, Jia *et al.* 2010) to investigate the effect of strain rate on consolidation yield stress (p_c), and all the tests showed that the value of p_c increases with the increase of strain rate in logarithm scale. Jia *et al.* (2010) reported that the value of coefficient of consolidation (c_v) increased with the increase of strain rate and the main reason is the increase of hydraulic conductivity.

Several theoretical studies have investigated how to obtain the c_v from CRS test results (Smith and Wahls 1969, Wissa *et al.* 1971, Umehara and Zen 1980, Lee 1981, Znidarcic *et al.* 1986). Consolidation theories can be categorized as either small-strain theory or large-strain theory, whose basic assumptions are different. However, only the small-strain theory is used in the standards for the CRS test (ASTM 2006, JSA 2000), because it is simple and easy to use. It is known that when the strain rate is high, the difference in strain distribution between the two theories for a given CRS test specimen is larger, and each of the two theories interprets different c_v

*Corresponding author, Ph.D., E-mail: jiarui@ilt.saga-u.ac.jp

small-strain theory can be used, and the conditions under which the large-strain theory yields better or more realistic results.

Ariake clay is a very soft clayey soil deposited around the Ariake Sea in Kyushu, Japan. In this study, undisturbed Ariake clay samples were subjected to CRS tests with strain rates of 0.002%/min, 0.02%/min and 0.2%/min. The small-strain and large-strain theories were employed to interpret c_v values from the test results, and the interpreted c_v values were compared. To provide a reference strain distribution within the specimen, the CRS tests were simulated by finite element method (FEM). For the specimen subjected to the CRS test, the strain distributions obtained by the small-strain theory and the large-strain theory were compared with the FEM results. Based on an analysis of the test and the simulation results, the applicable ranges of the small- and large-strain theories are suggested.

2. Experimental program

2.1 Soil samples

Undisturbed soil samples were obtained from three boreholes in Saga Plain of Kyushu Island, Japan, using a standard Japanese thin-walled sampler. In all, 10 tubes (each 1 m long) of sample were obtained at depths from 4.0 m to 21.0 m from the ground surface. After the sample tubes had been transported into the laboratory, soil samples were extruded from the thin-walled tube, sealed with wax and stored under water for CRS consolidation tests. The main clay mineral of Ariake clay is smectite (Ohtsubo *et al.* 1995). Fig. 1 shows the soil profile and some of the index properties of the soil samples from borehole-1 (BH-1). In the figure, C stands for clay, M for silt, S for sand, G for gravel, w_p for plastic limit, w_L for liquid limit and w_n for natural water content.

2.2 Test equipment and method

The equipment for the CRS test is illustrated in Fig. 2. The device consists of axial displacement control and back-pressure application systems. During each test, drainage was

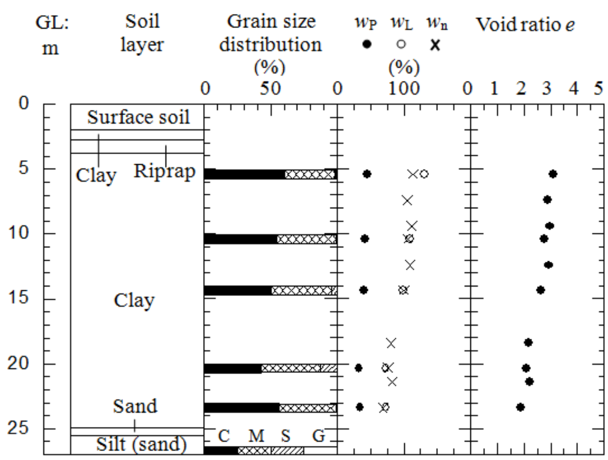

Fig. 1 Soil profile and some index properties (BH-1)

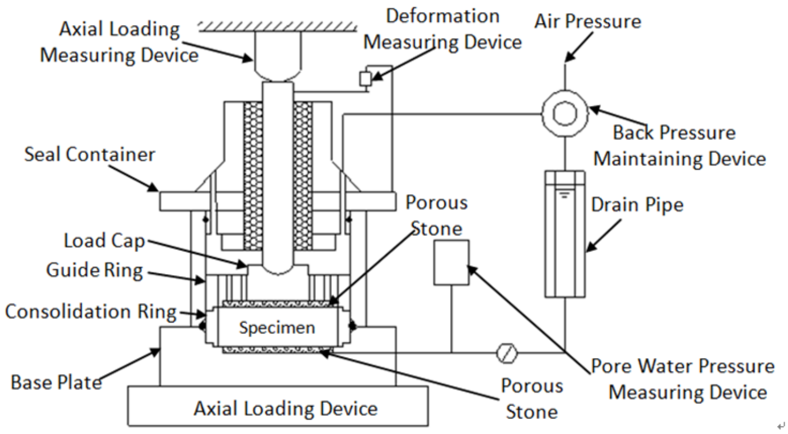

Fig. 2 The CRS test equipment

Table 1 Cases tested

Borehole	Depths* (m)	Strain rates (%/min)
BH-1	9.4, 12.4, 14.4, 21.4	0.002, 0.02, 0.2
BH-2	4.4, 11.4, 17.4, 20.9	0.002, 0.02, 0.2
BH-3	9.4, 20.4	0.002, 0.02, 0.2

*avg. depth of sample tube

allowed only at the top surface of the specimen. The axial displacement, axial load and excess pore water pressure at the bottom of the specimen were recorded through a data logger into a computer.

The CRS tests were carried out according to ASTM standard D 4186-06 (ASTM 2006). The soil specimens were 60 mm in diameter and 20 mm in nominal height. To increase the saturation, a back-pressure of 200 kPa was applied throughout the tests. For the CRS test, under the assumption that the distribution of excess pore water pressure within a specimen is parabolic (ASTM 2006), the average vertical effective stress σ_v' in a specimen was calculated as

$$\sigma_v' = \sigma_v - \frac{2}{3}u_b \tag{1}$$

where σ_v = the total vertical stress and u_b = the excess pore water pressure at the bottom of the specimen.

2.3 Cases tested

A total of 30 CRS tests were conducted for the undisturbed samples (Table 1). The soil samples were from 3 boreholes BH-1 to 3 located in a nearby area, and the soil profiles are similar as shown in Fig. 1. The strain rates used for the CRS tests were 0.002, 0.02 and 0.2%/min.

3. Theories for interpreting the coefficient of consolidation (cv)

3.1 Small-strain theory

In the case of the small-strain theory, the value of c_v can be calculated as follows (ASTM 2006)

$$c_v = \frac{\Delta\sigma_v \overline{H}^2}{2\overline{u}_b \Delta t} \tag{2}$$

where $\Delta\sigma_v$ = the total vertical stress increment in time interval Δt; $\overline{H}$ = the average specimen thickness and $\overline{u}_b$ = the average excess pore water pressure at the bottom of the specimen in time interval Δt.

3.2 Large-strain theory

The large-strain theory, which considers the changes in thickness of the specimen during consolidation, is governed by the following equation (Mikasa 1963)

$$\frac{\partial\zeta}{\partial t} = c_v \zeta^2 \frac{\partial^2\zeta}{\partial z_0^2} \tag{3}$$

where t = elapsed time; z_0 = the original coordinate for depth; e = the void ratio; e_0 = the initial void ratio and $\zeta = 1+e_0/1+e$, the consolidation ratio, which is related to the axial strain ε as $\zeta = 1/(1-\varepsilon)$.

Eq. (3) is a non-linear, second-order partial differential equation that cannot be solved explicitly, but can be easily solved numerically. With the initial and boundary conditions of the CRS test, for a given average strain ($\dot{\varepsilon}t = \Delta H_0/H_0$, where $\dot{\varepsilon}$ is the strain rate, H_0 is the initial specimen height and ΔH_0 is the specimen compression) and $c_v / \dot{\varepsilon}H_0^{\,2}$, a dimensionless parameter indicating the ratio between c_v and $\dot{\varepsilon}$, the ζ at any z_0 value within the specimen can be calculated by finite difference method.

The ratios of the strain at the bottom (ε_B) to that at the top (ε_T) of a specimen, $\varepsilon_B/\varepsilon_T$, under different average strains ($\dot{\varepsilon}t$) and $c_v / \dot{\varepsilon}H_0^{\,2}$ values are shown in Fig. 3, which forms the base for evaluating the c_v value from the CRS test results by the large-strain theory.

The change in void ratio Δe is proportional to the change in the vertical effective stress on a logarithmic scale, as follows

$$\Delta e = -C_c \log\left(\frac{\sigma_v' + \Delta\sigma_v'}{\sigma_v'}\right) \tag{4}$$

where C_c = compression index, which is assumed as a constant for the vertical effective stress from σ_v' to $\sigma_v' + \Delta\sigma_v'$. At other effective stress increments, C_c may change. In the overconsolidated range, C_c in the equation should be changed to swelling index (C_s).

Using the stress-strain relationship given by Eq. (4), the ratio of strain at the bottom of the specimen (ε_B) to that at the top of the specimen (ε_T) can be represented as

$$\frac{\varepsilon_B}{\varepsilon_T} = \frac{\log(\sigma_v - u_b) - \log(\sigma_{v0}')}{\log(\sigma_v) - \log(\sigma_{v0}')} \tag{5}$$

where σ_v = total vertical stress applied to the specimen; u_b = excess pore water pressure at the bottom of the specimen and σ'_{v0} = initial vertical effective stress.

CRS test measurements can be used in Eq. (5) to find $\varepsilon_B / \varepsilon_T$ for the corresponding $\dot{\varepsilon}t$ value. With $\varepsilon_B / \varepsilon_T$ and $\dot{\varepsilon}t$ known, a value of $c_v / \dot{\varepsilon} H_0^2$ can be obtained from Fig. 3; hence, c_v can be determined.

4. Test results and interpreted c_v values

4.1 Typical stress-strain-strain rate relation

Fig. 4 shows typical stress-strain-strain rate relationships for Ariake clay. The stress-strain curves shift rightward in a parallel manner with increases in strain rate, which is consistent with the results in the literatures (Vaid *et al.* 1979, Graham *et al.* 1983, Leroueil *et al.* 1985, Jia *et al.* 2010). Consolidation yield stress (p_c) increases with increases in strain rate. For all the soil samples tested in this study, p_c increases by about 18% with a tenfold increase in strain rate, which is within the typical range of strain rate effect on p_c of 10-20% (Graham *et al.* 1983) and is similar to the value reported by Jia *et al.* (2010). The curve in the virgin compression range shows nonlinearity due to the microstructured natural of Ariake clay (Chai *et al.* 2004).

4.2 Typical excess pore water pressure variations

Fig. 5 shows typical variation of excess pore water pressure at the bottom of the specimen (u_b) and pore water pressure ratio (the excess pore water pressure divided by the total vertical stress, u_b / σ_v). It can be seen that with the increase of the strain rate, u_b values was increased rapidly. To get a comparable result with the incremental loading consolidation test, it is recommended by ASTM (2006) that u_b / σ_v ratio should be in a range of 3% to 15%. Fig. 5(b) shows that for the strain rate of 0.2%/min, the maximum ratio was about 25% (larger than 15%) and for the strain rate of 0.002%/min, the ratio was less than 3%. Since the purpose of this study is to investigate the

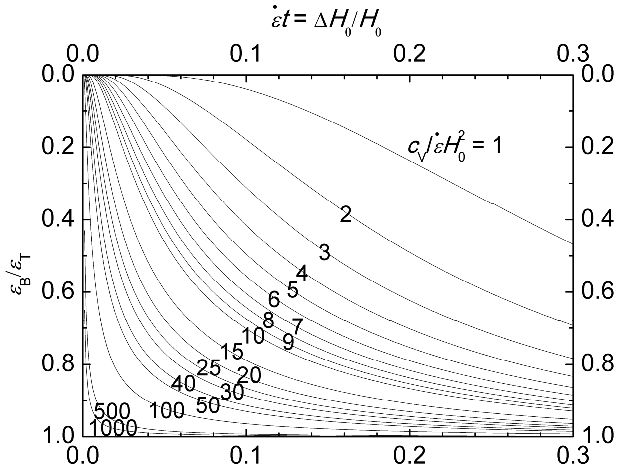

Fig. 3 Variations of $\varepsilon_B / \varepsilon_T$ (Large-strain theory)

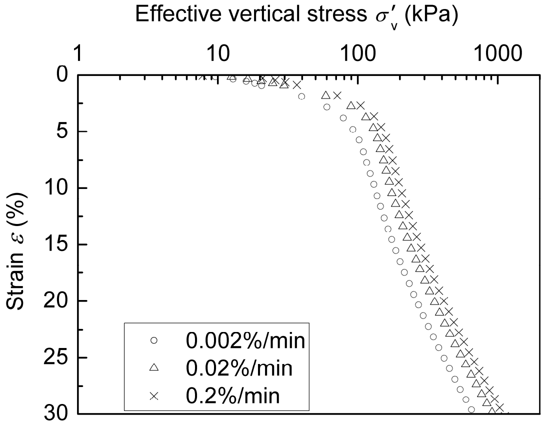

Fig. 4 Typical stress-strain-strain rate relation (BH-2, 17 - 17.8 m)

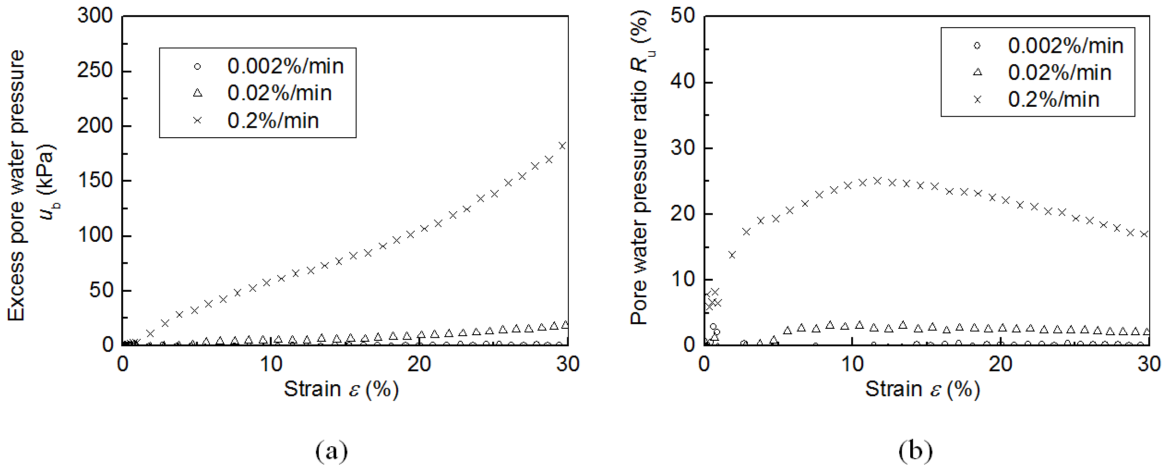

Fig. 5 Typical excess pore water variations: (a) u_b; and (b) u_b/σ_v

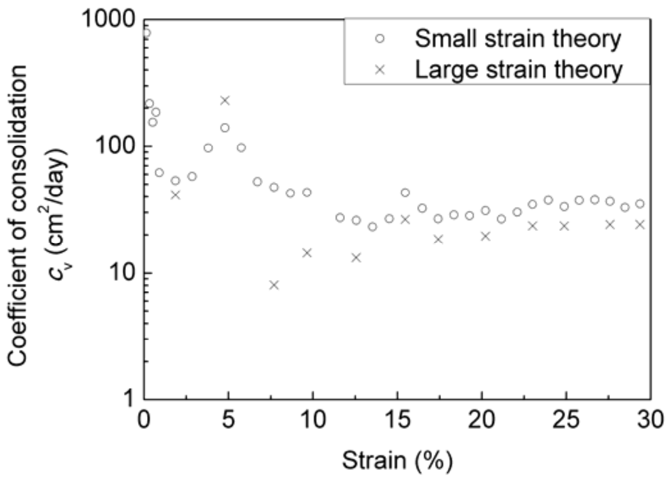

Fig. 6 Comparison of c_v ($\dot{\varepsilon}$ = 0.002%/min; 14 - 14.75 m)

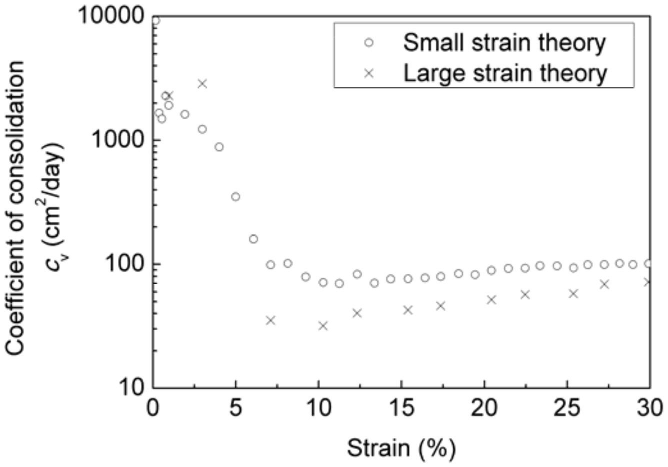

Fig. 7 Comparison of cv ($\dot{\varepsilon}$ = 0.02%/min; 14 - 14.75 m)

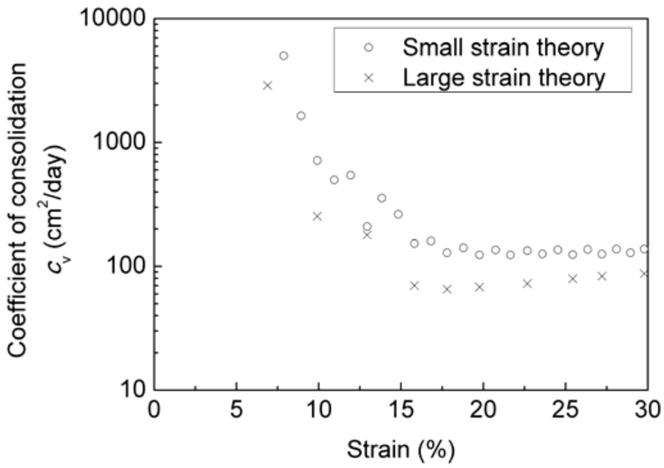

Fig. 8 Comparison of c_v ($\dot{\varepsilon}$ = 0.2%/min; 14 - 14.75 m)

suitable range of strain rate within which the small- and/or the large-strain theory can be used, a wide range of strain rate was adopted.

4.3 Comparison of the interpreted c_v values

For soil samples from BH-1 at 14 - 14.75 m depth, the c_v values interpreted by the small- and the large-strain theories are compared in Figs. 6, 7 and 8 for the strain rates of 0.002%/min, 0.02%/min and 0.2%/min, respectively. It can be seen that c_v values calculated by the large-strain theory are smaller than those by small-strain theory, and the discrepancy increases with the increases in the strain rate.

For all the soil samples tested, the values of c_v in the virgin compression range at average effective vertical stress $\overline{\sigma'_v}$ = 300 kPa at different depths are plotted in Figs. 9 and 10 for the strain rates of 0.002%/min and 0.2%/min, respectively. Generally the c_v values calculated by the large-strain theory are smaller than those by the small-strain theory, and although it is not quite obvious, the digital data show the discrepancy tends to increase with the increases in the strain rate.

4.4 Strain rate effect on c_v

The interpreted c_v values at $\overline{\sigma'_v}$ = 300 kPa are replotted in the form of normalized c_v versus normalized strain rate in Figs. 11 and 12 using the small-strain and the large-strain theories, respectively. The normalization was made by the c_v value at the strain rate of 0.02%/min. Although the data are scattered, in Figs. 11 and 12 there is a clear tendency for c_v to increase with the increases in the strain rate. The scatter of the data is partially due to that the different soil sample was used for different strain rate, and there might be spatial variation of undisturbed soil sample

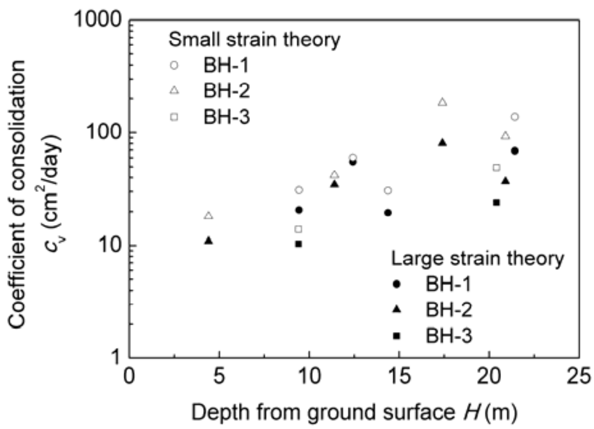

Fig. 9 Comparison of c_v (0.002%/min)

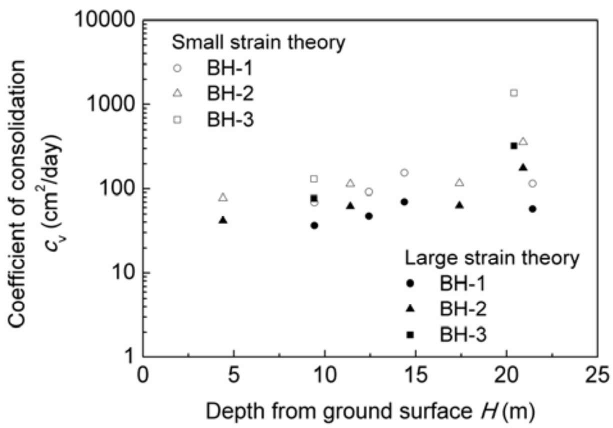

Fig. 10 Comparison of c_v (0.2%/min)

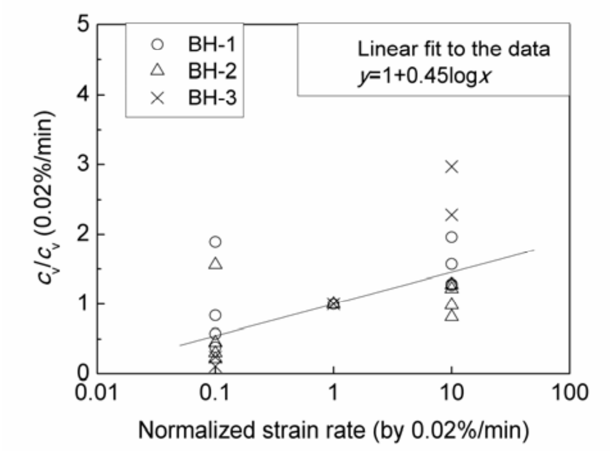

Fig. 11 Strain rate effect on cv (small-strain theory)

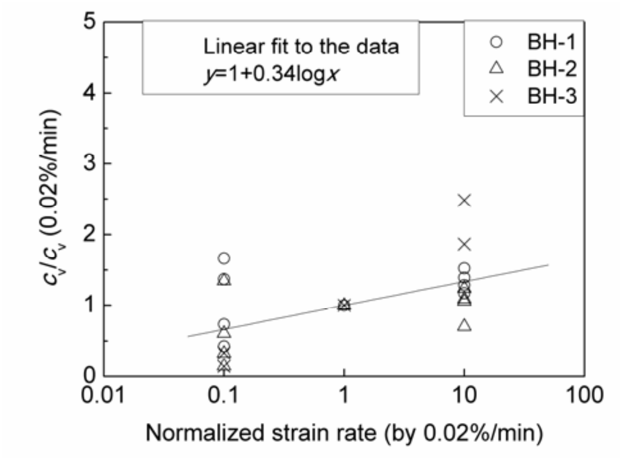

Fig. 12 Strain rate effect on c_v (large-strain theory)

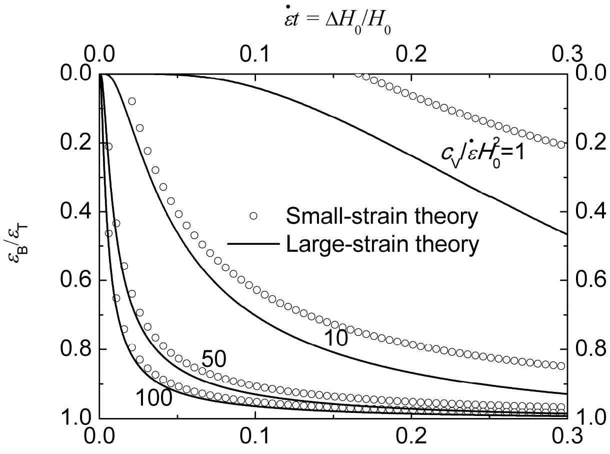

Fig. 13 Variations of $\varepsilon_B / \varepsilon_T$

within a sampling tube. With a tenfold increase in the strain rate, linear regression gives about a 45% increase in c_v in the case of using the small-strain theory and a 34% increase in c_v in the case of using the large-strain theory. So the large-strain theory results in a less strain rate effect on c_v than that of the small-strain theory.

5. Strain distributions within the specimen

5.1 Theoretical strain distributions

The strain distributions from the small- and the large-strain theories are compared in the plot of $\varepsilon_B / \varepsilon_T$ vs. $\Delta H_0 / H_0$ in Fig. 13. It can be seen that for given values of $\Delta H_0 / H_0$ and $\varepsilon_B / \varepsilon_T$, a smaller $c_v / \dot{\varepsilon} H_0^2$ value – and therefore a smaller c_v value – can be interpolated by the large-strain theory. For given $\Delta H_0 / H_0$ and $c_v / \dot{\varepsilon} H_0^2$ values, the small-strain theory will yield a smaller $\varepsilon_B / \varepsilon_T$ value and therefore a more non-uniform strain distribution within the specimen. It can also be seen that the difference increases with the increases in the strain rate (smaller $c_v / \dot{\varepsilon} H_0^2$ value), which is why the difference between the c_v values interpreted by the large-strain theory and the small-strain theory increase with the increases in the strain rate.

5.2 Numerical investigation of the strain distributions

It is desirable to determine which strain distribution, from the small-strain theory or the large-strain theory, is closer to the true strain distribution. However, it is very difficult to measure the true strain distribution within the specimen during the CRS test. So numerical analysis is used to estimate the true strain distribution.

In investigating the strain distribution pattern by numerical simulation, it is important to use a correct relationship between void ratio (e) and consolidation stress (p'). For most natural clay deposits (e.g., Ariake clay), in $e - \ln p'$ plot, the compression curves are non-linear (Fig. 4). Chai *et al.* (2004) found that in the $\ln(e + e_c) - \ln p'$ plot (e_c is a constant that depends on soil type), the compression curves are very close to linear for most natural clayey deposits. The linear $\ln(e + e_c) - \ln p'$ relationship was introduced into the Modified Cam Clay Model (Roscoe and Burland 1968) by Chai *et al.* (2004), which is used for numerical simulation in this study. The simulation program used was developed based on CRISP (Britto and Gunn 1987), which adopts a small strain formulation. The large deformation phenomenon is simulated by updating the node coordinates at the end of each step, i.e., an approximate updated lagrangian approach. In the case where there is no rotation of the elements, such as CRS test, the technique can correctly simulate the large deformation problem (Chai *et al.* 1995).

It has been found that the linear $\ln(e - 0.63) - \ln p'$ relationship accurately reproduces the $e - p'$ relation for Ariake clay (Jia and Chai 2010). The model parameter values adopted in this study are given in Table 2. The value of ν was assumed, and the other parameter values were determined based on laboratory test results.

The hydraulic conductivity listed in Table 2 is the initial value; during the consolidation it varied with e according to Taylor's equation (Taylor 1948)

$$k = k_0 10^{(e - e_0)/c_k} \tag{6}$$

where k_0 and k = hydraulic conductivities corresponding to e_0 and e, respectively, and c_k = a

Table 2 Parameters for finite element analysis

Description	ν	κ	λ	M	p'_y (kPa)	e_0	e_c	c_k	k_0 (m/day)	σ'_{v0} (kPa)
$\ln(e+e_c)-\ln p'$	0.3	0.05	0.30	1.2	42.5	3.51	-0.63	1.4	4.0E-04	20

Note: ν, Poisson's ratio; κ, slope of unloading-reloading line in the $\ln(e+e_c)-\ln p'$ plot; λ, slope of virgin consolidation line in the $\ln(e+e_c)-\ln p'$ plot; M, slope of critical state line in the q-p' plot (q is the deviator); p'_y, size of the yield locus; e_0, initial void ratio; k_0, initial hydraulic conductivity; σ'_{v0}, initial effective vertical stress.

constant that can be estimated as $0.4e_0$ (Tavenas *et al.* 1983).

The simulated strain distributions are compared with those obtained using the small- and the large-strain theories in Figs. 14, 15 and 16 for $c_v / \dot{\varepsilon}H_0^2$ = 1, 10 and 50 respectively. In the figures, $\bar{\varepsilon} = \dot{\varepsilon}t$ means average strain within the specimen. It can be seen that the strain distributions obtained by the large-strain theory closely correspond to the numerical simulations. The strain

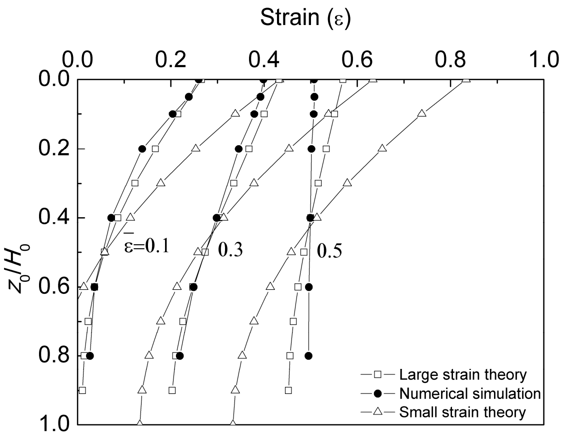

Fig. 14 Comparison of strain distribution ($c_v / \dot{\varepsilon}H_0^2$ = 1)

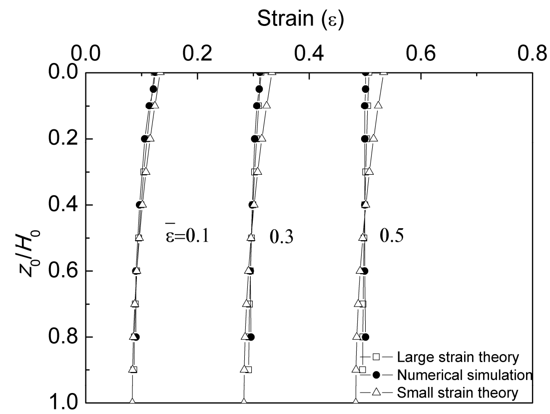

Fig. 15 Comparison of strain distribution ($c_v / \dot{\varepsilon}H_0^2$ = 10)

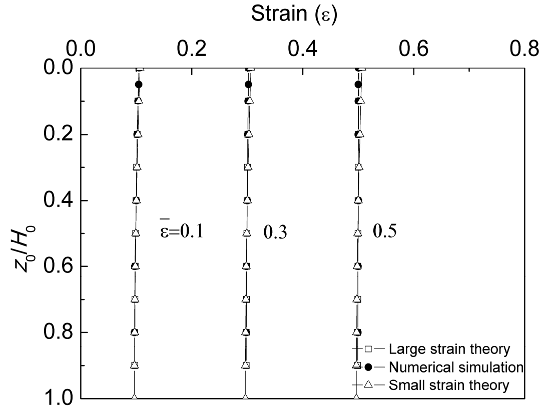

Fig. 16 Comparison of strain distribution ($c_v / \dot{\varepsilon} H_0^2$ = 50)

distributions obtained by the small-strain theory at higher strain rate ($c_v / \dot{\varepsilon} H_0^2$ = 1) are quite different from the numerical simulation results: They are more non-uniform. From Figs. 14 to 16, it can be observed that the small-strain theory can be used only for dimensionless parameter $c_v / \dot{\varepsilon} H_0^2 \geq 50$. c_v is about $1{\times}10^{-7}$ m^2/s for the undisturbed Ariake clay tested in this study, so $\dot{\varepsilon} \leq 0.03\%/\mathrm{min}$ results for the condition of $c_v / \dot{\varepsilon} H_0^2 \geq 50$. So it is suggested that the large-strain theory should be adopted for calculating c_v when $\dot{\varepsilon}$ > 0.03%/min for the undisturbed Ariake clay.

6. Conclusions

Based on the analysis of test and numerical simulation results, the following conclusions can be drawn.

(1) Small- and large-strain theories were adopted to interpret the value of the coefficient of consolidation (c_v) from CRS test results. It was clarified that the large-strain theory results in a smaller c_v value, and although it is not quite obvious, the digital data show a less strain rate effect on c_v than the small-strain theory.

(2) The small- and the large-strain theories result in different strain distributions within a soil specimen for a given average strain during the CRS test. The strain distributions obtained by the large-strain theory correspond closely to the numerical simulations (referred to as true distributions), and the strain distributions obtained by the small-strain theory at higher strain rates are quite different from those obtained by the numerical simulation.

(3) It is suggested that the small-strain theory can be used only for the condition of $c_v / \dot{\varepsilon} H_0^2 \geq 50$ ($\dot{\varepsilon}$ is strain rate and H_0 is specimen height). For undisturbed Ariake clay, it is recommended that the large-strain theory should be adopted for calculating the c_v value when $\dot{\varepsilon}$ > 0.03%/min.

References

ASTM Standard D 4186-06 (2006), *Standard Test Method for One-Dimensional Consolidation Properties of*

Saturated Cohesive Soils Using Controlled-Strain Loading, Annual Book of ASTM Standards, ASTM International, West Conshohocken, PA.

Bo, M.W., Choa, V. and Wong, K.S. (2010), "Constant rate of loading test on ultra-soft soil", *Geotech. Test. J.*, **33**(3), 1-9.

Bo, M.W., Wong, K.S. and Choa, V. (2008), "Constant rate of displacement test on ultra-soft soil", *Proceedings of the ICE - Geotechnical Engineering*, **161**(3), 129–135.

Britto, A.M. and Gunn, M.J. (1987), *Critical state soil mechanics via finite elements*, Ellis Horwood Limited, Chichester, UK.

Chai, J.C., Sakajo, S. and Yong, C.W. (1995), "Effect of soft subsoil settlement on embankment behavior", *Proceedings of 10th Asian Regional Conf. on Soil Mech. and Found. Eng*., Beijing, China, 158-159.

Chai, J.C., Miura, N., Zhu, H.H. and Yudhbir (2004), "Compression and consolidation characteristics of structured natural clay", *Can. Geotech. J.*, **41**(6), 1250-1258.

Graham, J., Crooks, J.H.A. and Bell, A.L. (1983), "Time effects on the stress-strain behaviour of natural soft clays", *Geotechnique*, **33**(3), 327-340.

Jia, R. and Chai, J.C. (2010), "Effect of strain distribution pattern on interpreting CRS consolidation test results", *Proceedings of the Fourth Japan-China Geotechnical Symposium*, Okinawa, Japan, 29-36.

Jia, R., Chai, J.C., Hino, T. and Hong, Z.S. (2010), "Strain-sate effect on consolidation behavior of Ariake clay", *Proceedings of the ICE - Geotechnical Engineering*, **163**(5), 267–277.

JSA (Japanese Standard Association) (2000) JIS A 1227, "Test method for one-dimensional consolidation properties of soils using constant rate of strain loading", JSA, Tokyo.

Lee, K. (1981), "Consolidation with constant rate of deformation", *Geotechnique*, **31**(2), 215-229.

Leroueil, S. (1988), "Tenth Canadian geotechnical colloquium: Recent developments in consolidation of natural clays", *Can. Geotech. J.*, **25**(1), 85-107.

Leroueil, S., Kabbaj, M., Tavenas, F. and Bouchard, R. (1985), "Stress-strain-strain rate relation for the compressibility of sensitive natural clays", *Geotechnique*, **35**(2), 159-180.

Mikasa, M. (1963), *The Consolidation of Soft Clay - A New Consolidation Theory and Its Application*, Kajima Institution Publishing Co., Ltd., Japan.

Moriwaki, T. and Satoh, T. (2009), "Method for determining the horizontal coefficient of permeability of clay", *Proceedings of the 44th Annual Presentation of Geotechnical Engineering*, Yokohama, Japan, 219-220. (in Japanese)

Ohtsubo, M., Egashira, K. and Kashima, K. (1995), "Depositional and post-depositional geochemistry and its correlation with geotechnical properties of the marine clays in Ariake Bay", *Geotechnique*, **45**(3), 509-523.

Roscoe, K.H. and Burland, J.B. (1968), "On the generalized stress-strain behavior of 'Wet' clay", *Engineering Plasticity*, *J. Heyman* and F.A. Leckie, eds., Cambridge University Press, Cambridge, U.K., 535-609.

Smith, R.E. and Wahls, H.E. (1969), "Consolidation under constant rates of strain", *J. Soil Mech. Found. Div.*, **95**(2), 519-539.

Tanaka, H., Udaka, K. and Nosaka, T. (2006), "Strain rate dependency of cohesive soils in consolidation settlement", *Soil. Found*., **46**(3), 315-322.

Tavenas, F., Jean, P., Leblond, P. and Leroueil, S. (1983), "The permeability of natural soft clays: Part II. Permeability characteristics", *Can. Geotech. J.*, **20**, 645-660.

Taylor, D.W. (1948), *Fundamentals of Soil Mechanics*, John Wiley and Sons, N.Y.

Terzaghi, K., Peck, R.B. and Mesri, G. (1996), *Soil Mechanics in Engineering Practice*, 3rd Edition, John Wiley and Sons, NY, USA

Umehara, Y. and Zen, K. (1980), "Constant rate of strain consolidation for very soft clayey soils", *Soil. Found*., **20**(2), 79-95.

Vaid, Y.P., Robertson P.K. and Campanella, R.G. (1979), "Strain rate behaviour of Saint-Jean-Vianney clay", *Can. Geotech. J.*, **16**(1), 34-42.

Wissa, A.E.Z., Christian, J.T., Davis, E.H. and Heiberg, S. (1971), "Consolidation at constant rate of strain", *J. Soil Mech. Found. Div.*, **97**(10), 1393-1413.

Yune, C.Y. and Chung, C.K. (2005), "Consolidation test at constant rate of strain for radial drainage", *Geotech. Test. J.*, **28**(1), 71-78.

Znidarcic, D., Schiffman, R.L., Pane, V., Croce, P., Ko, H.Y. and Olsen, H.W. (1986), "The theory of one-dimensional consolidation of saturated clays: Part V. Constant rate of deformation testing and analysis", G*eotechnique*, **36**(2), 227-237.

CC